 CMC, vol.36, no.3, pp.271-292, 2013

Theoretical Modeling of the Radiative Properties and Effective Thermal Conductivity of the Opacified Silica Aerogel

Zichun Yang[1,2,3], **Gaohui Su**[1,4], **Fengrui Sun**[1]

Abstract: In this paper, we investigate the radiative properties and the effective thermal conductivity (ETC) of the opacified silica aerogel by theoretical method. The radiative properties of the opacified silica aerogel are obtained by the modified Mie Scattering Theory that is used for particle scattering in absorbing medium. The modified gamma distribution is used to take account of the non-uniformity of the particle size. The solid thermal conductivity of the composite material is obtained by considering the scale effect of the particles. Based on these calculated thermophysical properties the coupled heat conduction and radiation through the evacuated opacified aerogel are solved by the finite volume method. And the radiation flux is computed by the P-1 approximation combined with the gray-band model. Results show that, the calculated thermophysical properties of the TiO_2-doped silica aerogel are close to the experimental data. The optimal mean radius for the largest radiation extinction of the SiC particles is about 1μm. The presented data of optimal doping amount of the SiC particles at different temperature conditions for the evacuated silica aerogel is very useful for thermal insulation material design.

Keywords: silica aerogel, radiative property, effective thermal conductivity, particle scattering

1 Introduction

SiO_2 aerogel is a typical super insulation material which provides a total thermal conductivity of about 0.020 W/(m·K) under ambient conditions [Wang et al (1995), Bouquerel et al (2012), Akimov (2003)]. It has great potential use in the aerospace

[1] Naval University of Engineering, China 430033.
[2] Huazhong University of Science and Technology, Wuhan, China 430074.
[3] Center for Aerospace Research & Education, University of California, Irvine Visiting professor.
[4] Corresponding author: su_gaohui@163.com

engineering, energy conservation, and etc. However, one problem will limit its application at high temperature as the SiO_2 material shows low radiation extinction for wavelength between 3-8 μm. A common method to reduce the radiative heat transfer at high temperature is loading opacifier to the aerogel matrix. It would be a tedious and expensive job to find an efficient opacifier and determine the optimal parameters for the opacifier by experiment. Theoretical model can provide guidelines for the material design and help to decrease the experiment work load [Li et al (2006), Dondero et al (2011)].

There are three heat transfer modes in the monolithic silica aerogel: gaseous conduction through the nanopores, solid conduction through the skeleton, and thermal radiation. The gaseous conduction can be negligible when the pressure is less than 1000 Pa [Zeng (1995)]. Heat transfer through the evacuated monolithic silica aerogel by coupled conduction and radiation. To solving this coupled heat transfer problem, one must first know the radiative properties and the thermal conductivity of the solid skeleton. The necessary radiative properties are absorption coefficient, scattering coefficient and scattering phase function. Zeng [Zeng (1995)] established a theoretical model to study the optimal doping amount of the carbon particles for the silica aerogel. In this pioneering work, Zeng estimated the absorption coefficient of the carbon particles by Rayleigh approximation because of the small size of these particles. Rayleigh approximation can be used only when the size parameter$x$ ($x = \pi d_p/\lambda$, d_p is the diameter of the particle, λ is the wavelength of the incident radiation) is far less than unity. When the particle size is comparable with the radiative wavelength, the Rayleigh approximation cannot be used. Mie scattering is an extension of the Rayleigh approximation for the scattering by homogeneous spherical particle in a non-absorbing medium with no restriction on the particle size [Modest (2003)]. Enguehard [Enguehard (2007)] computed the radiative properties of non-opacified and opacified silica particles using the Mie Scattering Theory. Han [Han et al (2009)] evaluated the radiative heat transfer in a randomly packed bed based on the geometric relations. Zhao [Zhao et al (2012)] computed the radiative properties of fiber-loaded silica aerogel using a modified anomalous diffraction theory (modified ADT) The modified ADT combines the geometric optics and Rayleigh approximation into a general expression to describe the radiative properties. It is an approximation of the Mie Scattering Theory. The diameter of the primary particle in the silica aerogel is about 2-5 nm [Dorcheh and Soleimani (2008)] which is far less than the thermal radiative wavelength that is between 0.1 μm and 100 μm [Modest (2003)]. Therefore, the scattering of the thermal radiation by the primary particles can be negligible and the radiation extinction caused by the aerogel is the pure absorption by the material. Radiation scattering by a spherical particle in a non-absorbing medium can be well explained

by the Mie theory. However, it needs to be modified when the medium is absorbing, because the host absorption not only attenuates the scattered wave in magnitude but also modulates the wave mode when the wave reaches the radiation zone [Yang et al (2002)]. Silica aerogel is an absorbing medium, thus, in order to obtain the radiative properties of a particle embedded in it, the absorption of the matrix should be taken into account.

Heat transfers through the monolithic silica aerogel by coupled conduction and radiation. The radiative transfer equation (RTE) is an integro-differential equation which is difficult to get the exact analytical solution. The problem becomes more complicated when radiation coupled with conduction as present in the silica aerogel. The solution of this coupled problem can be simplified by the diffusion approximation which is based on the optically thick assumption. However, when the radiation extinction coefficient is too small for some wave bands or the size of the material is too small, the optically thick assumption may be failed, and thus the diffusion approximation cannot be used.

A numerical calculating process is proposed in this paper to handle these problems. In order to take account of the effects of the absorption of the silica aerogel matrix on the radiative properties of the loaded particle, the modified Mie Scattering Theory for absorbing medium particles is introduced. Based on the calculated thermophysical properties, the coupled conduction and radiation heat transfer is solved by the finite volume method combined with the P-1 radiation model. The optimal parameters of the opacifier can be used as the reference data for thermal insulation design.

2 Radiative properties

The opacifier in the aerogel matrix is clouds of particles with nonuniform size. The radiative properties of a single particle were first calculated using the modified Mie scattering theory. Then, the radiative properties of the opacified aerogel were obtained based on the radiative properties of a single particle and the absorption coefficient of the silica matrix.

2.1 Radiative properties of a single particle

Two approaches are usually used to study the radiative properties of a single particle in embedded an absorbing medium: the Far Field Approximation (FFA) and the Near Field Approximation (NFA) [Randrianalisoa et al (2002)]. The FFA [Yin and Pilon (2006)] is based on the asymptotic form of the electromagnetic field in the radiation zone far from the scatterer. The NFA [Fu and Sun (2001)] is based on the information of the electromagnetic field at the particle surface. In this study, the

scattering efficiency and the scattering phase function of the opacifier particle were calculated by the FFA, and the absorption efficiency of the opacifier particle was calculated by the NFA.

2.1.1 *Efficiencies of a single particle*

The opacifier particle was assumed to be spherical; the scattering efficiency Q_{sca} of a spherical particle embedded in the silica aerogel matrix was calculated using the following formula derived from the FFA:

$$Q_{\mathrm{sca}} = \frac{4k_0^2 \exp(-2k_0 x)}{\left(n_0^2 + k_0^2\right)\left[1 + (2k_0 x - 1)\exp(2k_0 x)\right]} \sum_{n=1}^{\infty} (2n+1)\left(|a_n|^2 + |b_n|^2\right) \tag{1}$$

Where n_0 is the refractive index of the aerogel matrix n=1+0.00019ρ, ρ_0 is the apparent density of the aerogel matrix k is the absorption index of the aerogel matrix which is derived from the absorption coefficient of the aerogel matrix $\alpha_{\lambda,0}$, k=$\lambda\,\alpha_{\lambda,0}/4\pi\ \alpha_{\lambda,0}$ is the experimental data [Fricke et al (2008)]. The Mie coefficients a_n, b_n were obtained by the following recursive relations:

$$a_n = \frac{\left[m_0 D_n(m_1 x)/m_1 + n/(m_0 x)\right]\psi_n(m_0 x) - \psi_{n-1}(m_0 x)}{\left[m_0 D_n(m_1 x)/m_1 + n/(m_0 x)\right]\xi_n(m_0 x) - \xi_{n-1}(m_0 x)} \tag{2}$$

$$b_n = \frac{\left[m_1 D_n(m_1 x)/m_0 + n/(m_0 x)\right]\psi_n(m_0 x) - \psi_{n-1}(m_0 x)}{\left[m_1 D_n(m_1 x)/m_0 + n/(m_0 x)\right]\xi_n(m_0 x) - \xi_{n-1}(m_0 x)} \tag{3}$$

In which, $m_0 = n_0 + \mathrm{i}k_0$ is the complex refractive index of the aerogel matrix $m_1 = n_1 + \mathrm{i}k_1$ is the complex refractive index of the opacifier particle. $\psi_n(z)$, $\xi_n(z)$ are the Riccati-Bessel functions with respect to the argument z. $D_n(z)$ is the logarithmic derivative of $\psi_n(z)$ The index n is truncated at a maximum n_{max} proposed by Bohren and Huffman [Bohren and Huffman (1983)]:

$$n_{\max} = x + 4x^{1/3} + 2 \tag{4}$$

The absorption efficiency Q_{abs} of a spherical particle embedded in the silica aerogel matrix was calculated using the following formula derived from the NFA

$$Q_{\mathrm{abs}} = \frac{8\pi k_0^2}{n_0[1 + (2k_0 x - 1)\exp(2k_0 x)]} \sum_{n=1}^{\infty} (2n+1)\mathrm{Im}(A_n) \tag{5}$$

In which, $\mathrm{Im}(A_n)$ refers to the imaginary part of the complex coefficient A_n. A_n was given by

$$A_n = \frac{|c_n|^2 \psi_n(m_1 x)\psi_n'^{*}(m_1 x) - |d_n|^2 \psi_n'(m_1 x)\psi_n'^{*}(m_1 x)}{2\pi m_1} \tag{6}$$

Here, the asterisk denotes the complex conjugate, $\psi_n'(z)$ is the derivative of $\psi_n(z)$. The Mie coefficients c_n, d_n were obtained by the following recursive relations:

$$c_n = \frac{m_1 \xi_n(m_0 x)\,\psi_n'(m_0 x) - m_1 \xi_n'(m_0 x)\,\psi_n(m_0 x)}{m_1 \xi_n(m_0 x)\,\psi_n'(m_1 x) - m_0 \xi_n'(m_0 x)\,\psi_n(m_1 x)} \tag{7}$$

$$d_n = \frac{m_1 \xi_n'(m_0 x)\,\psi_n(m_0 x) - m_1 \xi_n(m_0 x)\,\psi_n'(m_0 x)}{m_1 \xi_n'(m_0 x)\,\psi_n(m_1 x) - m_0 \xi_n(m_0 x)\,\psi_n'(m_1 x)} \tag{8}$$

2.1.2 Scattering phase function of a single particle

The scattering phase function of a single particle embedded in an absorbing matrix takes the same form as that in a non-absorbing matrix and is given by:

$$\Phi_\lambda(\Theta) = \frac{|S_1|^2 + |S_2|^2}{\sum_{n=1}^{\infty}(2n+1)\left(|a_n|^2 + |b_n|^2\right)} \tag{9}$$

In which, the amplitude scattering function $S_1$and S_2 are calculated by

$$S_1(\Theta) = \sum_{n=1}^{\infty} \frac{2n+1}{n(n+1)} \left[a_n \pi_n(\cos\Theta) + b_n \tau_n(\cos\Theta)\right] \tag{10}$$

$$S_2(\Theta) = \sum_{n=1}^{\infty} \frac{2n+1}{n(n+1)} \left[b_n \pi_n(\cos\Theta) + a_n \tau_n(\cos\Theta)\right] \tag{11}$$

Where Θ is the scattering angle, $\pi_n(\cos\Theta)$, $\tau_n(\cos\Theta)$ describe the angular scattering patterns of the spherical harmonics [Bohren and Huffman (1983)].

2.2 Radiative properties of the opacified silica aerogel

2.2.1 Effective coefficients of opacified silica aerogel

The opacified silica aerogel is heterogeneous media which consist of the aerogel matrix and the opacifier particles. It was treated as homogenous media in this study and used the effective radiative properties to calculate the radiative heat transfer. The effective radiative properties are determined by the efficiencies of the doped particles and the absorption coefficient of the silica matrix. The effective scattering coefficient $\sigma_{\lambda,\mathrm{eff}}$ and the effective absorption coefficient $\alpha_{\lambda,\mathrm{eff}}$ were calculated based on the independent scattering assumption:

$$\sigma_{\lambda,\mathrm{eff}} = n_t \int_0^{\infty} \pi r^2 Q_{\mathrm{sca}}(r)\, f(r) dr \tag{12}$$

$$\alpha_{\lambda,\text{eff}} = \alpha_{\lambda,0} + n_t \int_0^\infty \pi r^2 \left[Q_{\text{abs},1}(r) - Q_{\text{abs},0}(r) \right] f(r) dr \tag{13}$$

Where n_t is the number of particle per unit volume$r$ is the radius of the particle $f(r)$ is the particle distribution function and $f(r)dr$ defined as the number percentage of particle with radius between r and r+dr $Q_{\text{abs},1}$ is the absorption efficiency of the particle, $Q_{\text{abs},0}$ is the absorption efficiency of the particle which has the identical complex refraction index with the matrix. In order to study the opacification effect of a single particle in the absorbing medium, the $(Q_{\text{abs},1} - Q_{\text{abs},0})$ and $(Q_{\text{sca}} + Q_{\text{abs},1} - Q_{\text{abs},0})$ were defined as the effective absorption efficiency and effective extinction efficiency, respectively, in this paper.

The effective extinction coefficient $\beta_{\lambda,\text{eff}}$ and the scattering albedo ω_λ of the opacified silica aerogel thus can be obtained:

$$\beta_{\lambda,\text{eff}} = \sigma_{\lambda,\text{eff}} + \alpha_{\lambda,\text{eff}} \tag{14}$$

$$\omega_\lambda = \frac{\sigma_{\lambda,\text{eff}}}{\beta_{\lambda,\text{eff}}} \tag{15}$$

The effective specific coefficients are defined as the ratio of the effective coefficients to the apparent density of the composite aerogel ρ_2: $\sigma_{\lambda,\text{m,eff}=}\sigma_{\lambda,\text{eff}}/\rho_2$, $\alpha_{\lambda,\text{m,eff}=}\alpha_{\lambda,\text{eff}}/\rho_2$, $\beta_{\lambda,\text{m,eff}}=\beta_{\lambda,\text{eff}}/\rho_2$ The aerogel matrix density ρ_0, the opacifier density ρ_1 the composite aerogel density ρ_2 and the mass fraction of the opacifier w have a relation as

$$\rho_2 = \frac{\rho_1 \rho_0}{\rho_1 + (\rho_0 - \rho_1) w} \tag{16}$$

2.2.2 *Scattering phase function of the opacified silica aerogel*

For nonuniform particles in the aerogel matrix, the scattering phase function is not the same for all particles. It follows that the scattered energies into a given direction must be summed over all particles and then normalized. It can be estimated by [Modest (2003)]:

$$\overline{\Phi_\lambda(\Theta)} = \frac{\int_0^\infty \Phi_\lambda(\Theta) \sigma_{\lambda,\text{eff}} f(r) dr}{\int_0^\infty \sigma_{\lambda,\text{eff}} f(r) dr} \tag{17}$$

The asymmetry factor is calculated as

$$g_\lambda = \frac{1}{2} \int_0^\pi \overline{\Phi_\lambda(\Theta)} \cos\Theta \sin\Theta \mathrm{d}\Theta \tag{18}$$

2.2.3 Particle distribution function

A number of different function forms have been used to describe the size distribution for clouds of particles with nonuniform radius The modified gamma distribution was used here

$$f(r) = Cr^{\gamma} \exp\left(-Br^{\delta}\right) \tag{19}$$

In which, the four constants C, B, γ and δ are positive and real, γ and δ are usually chosen to be integers. As the values of γ and δ increase, the particle size distribution becomes more concentrated. C, B are given by

$$B = \frac{1}{r_{\mathrm{m}}^{\delta}} \left[\Gamma\left(\frac{\gamma+4}{\delta}\right)\right]^{\frac{\delta}{3}} \left[\Gamma\left(\frac{\gamma+1}{\delta}\right)\right]^{-\frac{\delta}{3}} \tag{20}$$

$$C = \frac{\delta}{r_{\mathrm{m}}^{\gamma+1}} \left[\Gamma\left(\frac{\gamma+4}{\delta}\right)\right]^{\frac{\gamma+1}{3}} \left[\Gamma\left(\frac{\gamma+1}{\delta}\right)\right]^{-\frac{\gamma+4}{3}} \tag{21}$$

Where Γ is the gamma function, r_m is the mean radius of the particles which can be estimated by the volume fraction f_v and n_t according to the following formula

$$r_{\mathrm{m}} = \left(\frac{3f_v}{4\pi n_t}\right)^{\frac{1}{3}} \tag{22}$$

3 Solid thermal conductivity

The extremely high porosity (80-99.8%) and very small primary particle size (2-5nm) of the silica aerogel lead to a very low solid thermal conductivity. Zeng [Zeng et al (1995)] studied the heat transfer through the aerogel by replacing the random structure of the skeleton with a regular structure and proposed three geometric structures (intersecting square rod, intersecting cylindrical rod, and intersecting spherical structure) for the thermal conductivity calculating Wei [Wei (2011)] calculated the solid thermal conductivity of the aerogel skeleton using the intersecting spherical structure. Coquard [Coquard (2013)] estimated the magnitude of the conductive heat transfer inside the nano-structured silica using a realistic representation of the porous structure. The solid thermal conductivity k_s of monolithic silica aerogel strongly depends on the density. A relation between the k_s and the density based on the experimental data has been used widely and is expressed as [Lu et al (1992), Zhao (2012), Wang (1995)]

$$k_{\mathrm{s}} = c_0 \rho_0^{\alpha} \tag{23}$$

Where α=1.5, c_0 is independent of the density. The solid conductivity of pure silica aerogel is about 0.0035 W/(m·K) when the density is 100 kg/m^3 [Zeng (1995)]. Therefore, c_0 is about 3.5×10^{-6}. To take account of the effect of loading opacifier on the solid conductivity this relation should be modified as

$$k_{\mathrm{s}} = c_0\left(1+f\frac{k_{\mathrm{par}}}{k_{\mathrm{siO_2}}}\right)\rho_2^{\alpha} \tag{24}$$

In which, f is the ratio of the volume of the doped particles to the volume of matrix in the opacified aerogel. $k_{\mathrm{siO_2}}$is the thermal conductivity of amorphous SiO_2[Zhao (2012)]

$$k_{\mathrm{siO_2}}(T) = 7.5264\times10^{-1}+3.1286\times10^{-3}T-4.5242\times10^{-6}T^2+3.5253\times10^{-9}T^3 \tag{25}$$

k_{par} is the thermal conductivity of the opacifier particle. Because of the small dimension of the particles, the thermal conductivity may show scale effect [Ni et al (2011)]. The dominant heat carriers in dielectric solid materials are phonons [Tian and Yang (2008), Chen et al (2011)]. The kinetic theory was used to estimate the thermal conductivity of the particles [Huang et al (2009)]

$$k_{\mathrm{par}} = \frac{1}{3}Cv_{\mathrm{m}}l_{\mathrm{par}} \tag{26}$$

In which C is the specific heat of the bulk material. v_m is the mean sound velocity of the bulk material. The mean free path (MFP)of phonons in the particle, l_{par}, is estimated by the Matthiessen rule [Chen (2005)]. v_m and l_{par} are given by

$$v_{\mathrm{m}} = \left[\frac{1}{3}\left(\frac{1}{v_{\mathrm{l}}^3}+\frac{2}{v_{\mathrm{t}}^3}\right)\right]^{-\frac{1}{3}} \tag{27}$$

$$\frac{1}{l_{\mathrm{par}}} = \frac{1}{l_{\mathrm{bulk}}}+\frac{1}{d_{\mathrm{mp}}} \tag{28}$$

In which v_{l} and v_{t} are the longitudinal and transverse sound velocities respectively. d_{mp} is the mean diameter of the particles. l_{bulk} is the MFP of phonons in the bulk material, which was estimated by the thermal conductivity of the bulk material k_{bulk}

$$l_{\mathrm{bulk}} = \frac{3k_{\mathrm{bulk}}}{Cv_{\mathrm{m}}} \tag{29}$$

4 Heat transfer

4.1 Heat transfer model

A commonly used model to calculate the gaseous conductivity k_g in the nanoporous aerogel is expressed as [Zeng (1995), Wei et al (2012)]

$$k_{\mathrm{g}} = \frac{60.22pT^{-0.5}\Pi}{0.25S_{\mathrm{s}}\rho_2\Pi^{-1} + 4.01\times10^4 pT^{-1}} \tag{30}$$

In which, Π is the porosity of the aerogel, p is the pressure, S_{s} is the specific surface area defined as surface area per unit mass, which can be determined by the BET measurement [Liang et al (2009)]. This model shows that the specific surface area has an important impact on the gaseous conductivity. For example, under ambient conditions, assuming ρ_2 is 200 kg/m^3 and Π is 0.90, when the S_{s} is 500,000 m^2/kg, k_{g} is about 0.0077 W/(m·K); when the S_{s} is 1000,000 m^2/kg, k_{g} is about 0.0046 W/(m·K). Experimental data show that doping particles in aerogel would reduce the S_{s} [Zhang and Fang (2012)], but there are not enough data to determine the relation between the loading amount and the specific surface area. Thus the effect of loading opacifier on the gaseous conductivity cannot be described precisely. In order to obtain more accurate quantitative results of the effect of loading opacifier on the thermal properties of silica aerogel, heat transfer through the evacuated monolithic silica aerogel was studied in this research.

Heat transfers through the evacuated monolithic silica aerogel by coupled conduction and radiation. A 2-D heat transfer model was analyzed in this study. The steady-state energy equation for coupled conduction and radiation can be written as

$$\nabla\cdot(k_s\nabla T) - \nabla\cdot q_r = 0 \tag{31}$$

With the boundary conditions

$$T(y,0) = T_c; T(y,L_z) = T_h; \left.\frac{\partial T}{\partial y}\right|_{y=0} = 0; \left.\frac{\partial T}{\partial y}\right|_{y=L_y} = 0 \tag{32}$$

Where q_r is the radiative heat flux, T_c is the temperature of the cold wall and T_h is the temperature of the hot wall. L_y, L_z are the dimensions of the computational domain. The physical model is shown in Fig. 1. All boundaries were set as diffuse gray surfaces, and the emissivity of the hot and the cold wall were set to unity, the emissivity of the left and right walls were set to zero.

The energy equation was solved by the finite volume method based on the commercial software ANSYS-FLUENT. The ANSYS-FLUENT provides five radiation

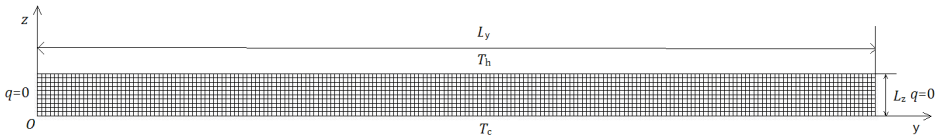

Figure 1: Schematic diagram of the physical model

models to include radiation in the energy equation, the Discrete Transfer Radiation Model (DTRM), the P-1 radiation model, the Rosseland radiation model (diffusion approximation), the Discrete Ordinates (DO) radiation Model, and the Surface-to-Surface (S2S) radiation model. In which, the former four models can calculate the radiative heat transfer within a participating medium. Only the P-1 radiation model and the DO radiation model can be used when the extinction coefficient of the medium varies dramatically with the wavelength just as the silica aerogel displays. It was found that the P-1 radiation model and the Rosseland radiation model gave a very close value of the heat flux when the optically thickness is large. However, the DO radiation model tended to over-predict that value. Therefore, the P-1 radiation model was used in this study to calculate the radiative heat transfer. The nongray effective extinction coefficient of the aerogel was treated by the gray-band model.

In order to deal with the isotropic property of the opacified aerogel, the isotropic scaling was used. The scaling effective extinction coefficient $\beta_{\lambda,\mathrm{eff}}^{\mathrm{scal}}$ is calculated by:

$$\beta_{\lambda,\mathrm{eff}}^{\mathrm{scal}} = \beta_{\lambda,\mathrm{eff}}\left(1 - g_\lambda \omega_\lambda\right) \tag{33}$$

And the scaling effective specific extinction coefficient can be easily obtained: $\beta_{\lambda,\mathrm{m,eff}}^{\mathrm{scal}} = \beta_{\lambda,\mathrm{eff}}^{\mathrm{scal}} \Big/ \rho_2$

4.2 Effective thermal conductivity

After the results converged, the heat flux of the hot wall q_h and cold wall q_c were extracted. The ETC of the evacuated silica aerogel k_eff can be readily calculated by the Fourier's law of heat conduction [Incropera et al (2007), Liu (2011)]:

$$k_\mathrm{eff} = \frac{L_z\left(q_\mathrm{h} - q_\mathrm{c}\right)}{2\left(T_\mathrm{h} - T_\mathrm{c}\right)} \tag{34}$$

Where, the q_h is positive as indicates heat flowing into the computational domain, the q_c is negative as indicates heat flowing out the computational domain.

5 Application and discussion

5.1 TiO_2-doped silica aerogel

Because of the oxidation of carbon in air at high temperature, the carbon-doped aerogel can be used only up to 300°C in oxygen atmosphere. In order to search for more efficient opacifier for silica aerogel, Kuhn investigated various minerals by experimental method [Kuhn et al (1995)] The radiative properties and ETC of the TiO_2-doped silica aerogel have been measured [Kuhn et al (1995), Wang et al (1995)]. These thermophysical properties were also calculated by the theoretical model proposed in this study.

5.1.1 Radiative properties of the TiO_2-doped silica aerogel

Fig. 2 shows the calculated value and the experimental value (with an accuracy of about 12%) of the scaling effective specific extinction coefficient of the TiO_2-doped silica aerogel [Kuhn et al (1995)]. w=0% refers to the pure silica aerogel. The mean radius of the TiO_2 particles r_m=1.75 μm The distribution constants γ=δ=16 The complex index and density of the TiO_2 material, m_1=2.71+ 0i, ρ_1= 4230 kg/m^3. The density of the silica matrix, ρ_0=185.41 kg/m^3. As shown in Fig. 2, the calculated results are close to the experimental results. The opacification effect of doping TiO_2 particles on the radiation are mainly reflected in the wavelength between 2-9 μm. The reason is that particles with a given size can only scatter the radiation within corresponding wave band. As shown in Fig. 3, the effective extinction efficiency for a single TiO_2 particle with a radius of 1.75 μm shows positive value mainly for wavelength below than 10 μm.

The difference between the calculated value and the experimental value in Fig. 2 may be attributed to the unknown size distribution form of the opacifier particles used in the experiment. Fig. 4 shows the effect of the distribution constants in the modified gamma distribution on the radiative properties of TiO_2doped silica aerogel. It can be seen that the size distribution of the particles may have important effect on the radiative properties If the distribution of the particle size is more dispersed (γ=δ=2) the variation of the radiative properties versus wavelength is much more gentle Fig. 4(a) shows that the particle size distribution has little effect on the effective absorption coefficient but can affect the effective scattering coefficient which dominate the effective extinction coefficient for the wavelength below 10 μm. Fig. 4(b) shows that the asymmetry factor is positive through the considered wavelength range which means more radiation will be scattered into the forward direction Fig. 5 is the scattering phase function of the TiO_2-doped silica aerogel, in which a very strong forward scattering can be seen

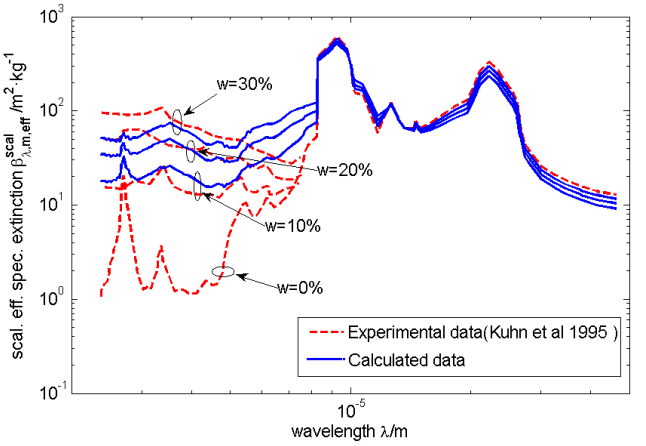

Figure 2: Dependence of the scaling effective specific extinction coefficient versus wavelength of TiO_2-doped silica aerogel on amount of the TiO_2, calculated data and experiment data

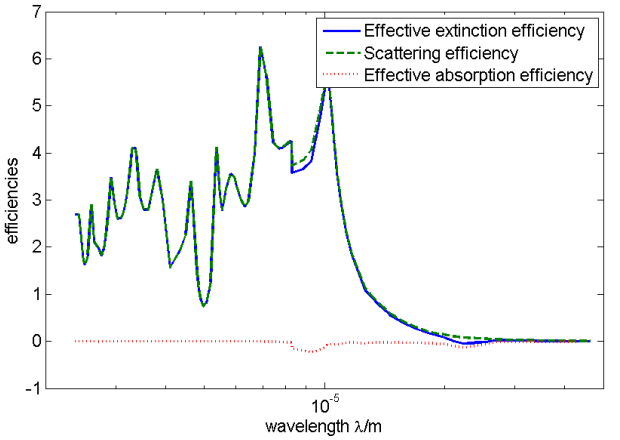

Figure 3: Dependence of the effective efficiency versus wavelength of a single TiO_2 particle embedded in silica aerogel matrix

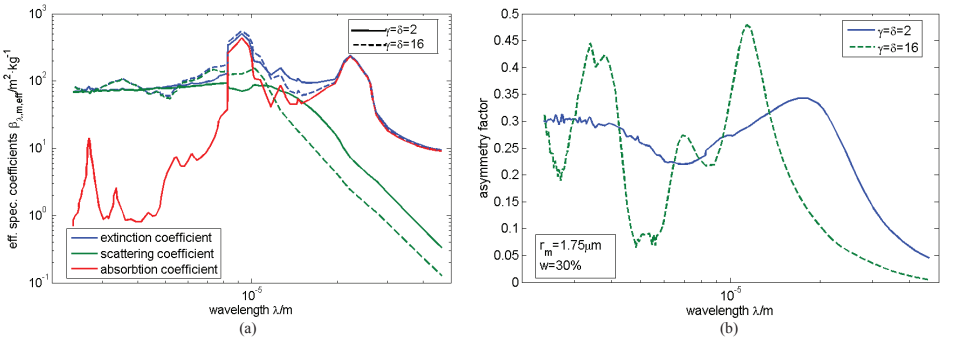

Figure 4: Dependence of the radiative properties versus wavelength of TiO_2 doped silica aerogel on distribution constants, (a) effective specific extinction coefficient; (b) asymmetry factor

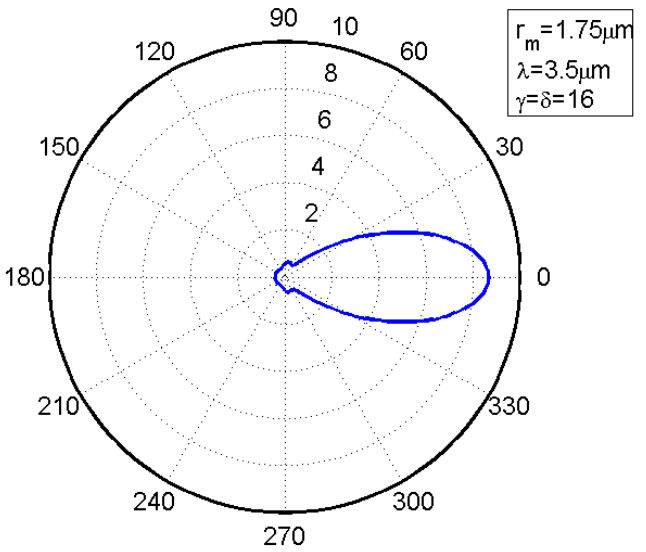

Figure 5: Scattering phase function of the TiO_2 doped silica aerogel

5.1.2 Thermal conductivity of the TiO_2 particle

The thermal conductivity of bulk TiO_2 material and TiO_2 particle with a radius of 1.75 μm is shown in Fig. 6. The latter was estimated by the Eq. 27 The specific heat and thermal conductivity of the bulk TiO_2 were taken from the reference [Incropera et al (2007)]. And the longitudinal and transverse sound velocities were, v_l=10327 m/s, v_t=5500 m/s [Caravaca et al (2009)]. It can be seen that the particle thermal conductivity is lower than that of the bulk material because the micron size of the particle are comparable to the MFP of the phonons in the bulk material (about 5.776 μm at 300K).

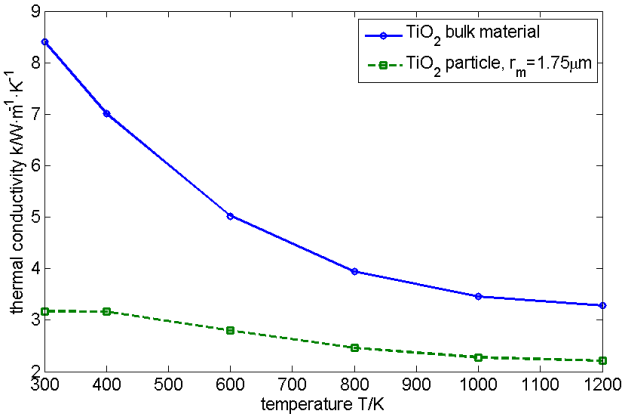

Figure 6: Dependence of thermal conductivity of bulk TiO_2 and TiO_2 particle versus temperature

5.1.3 ETC of the TiO_2-doped silica aerogel

The ETC of the evacuated TiO_2-doped silica aerogel under different temperatures were calculated. The mass fraction of the TiO_2 particles is 30%, the density of the composite is 260 kg/m^3 and the distribution constants γ and δ are 16 The results are shown in Fig. 7 by the green dashed line. The abscissa represents the average temperature, $(T_h + T_c)/2$, with $T_h T_c$=60 K. The measured ETC of the non-evacuated silica aerogel with a density 260 kg/m^3 doped with 30% TiO_2 and 3% ceramic fiber are shown in Fig.7 by the red circle [Wang et al (1995)]. The measured gaseous conductivity was 0.010 W/(m·K). In order to evaluate the results computed by this research, the measured gaseous conductivity was added to the calculated ETC for evacuated state and the total ETC for the non-evacuated TiO_2-doped silica aerogel were obtained, as shown in Fig. 7 by the blue solid line. It can be seen that, the

calculated value are close to the experimental value. As the temperature increases, the difference between them become larger, the maximum relative error is about 12.4% within the investigated temperature range. This difference comes from the different effective extinction coefficient. The additional 3% ceramic fiber in the experimental material may exacerbate the agglomeration of the TiO_2 particles which reduces the scattering cross-section due to the effect of dependent scattering and leads to a reduced effective extinction coefficient.

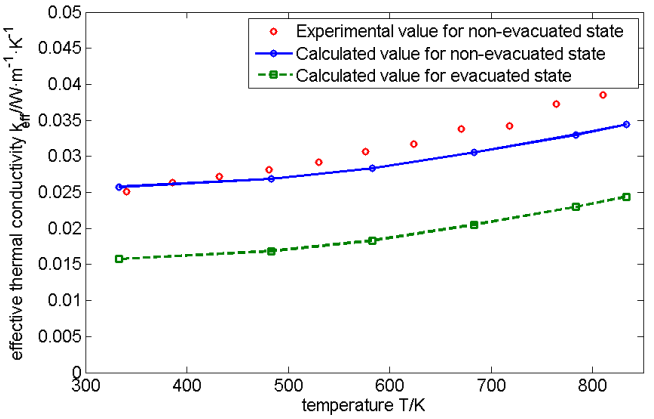

Figure 7: Dependence of the ETC of TiO_2 doped silica aerogel versus temperature, calculated data and experiment data

5.2 SiC-doped silica aerogel

Because of the high refractive index, stability at high temperature and low price, the SiC particles can be used as an efficient opacifier [Yang and Chen (2009)]. However, the thermal conductivity of the bulk SiC material is very high, about 490 W/(m·K) at 300 K. Loading SiC powders to the silica aerogel matrix can reduce the radiative heat transfer but also increase the solid conductivity. Therefore, there may be an optimal loading amount of the SiC particles which provides a better insulating performance for the silica aerogel.

5.2.1 Radiative properties of SiC-doped silica aerogel

Fig.8 shows the variation of the scaling effective specific extinction coefficient of the SiC-doped silica aerogel versus the mean radius of the SiC particles. The complex index and density of the bulk SiC are 2.486+0.043i and 3214 kg/m^3, respectively. The results show that the scaling effective specific extinction obtains a max-

imum value when the mean radius is about 1μm. Fig. 9 is the calculated scaling effective specific extinction coefficient of the SiC-doped silica aerogel under different doping amount. The mean radius of the doped SiC particles is 1μm and the distribution constants γ and δ are 2.

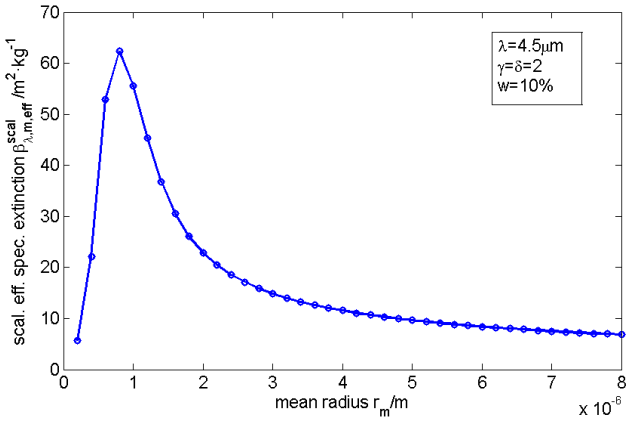

Figure 8: Dependence of the scaling effective specific extinction coefficient of SiC-doped silica aerogel versus mean radius of the SiC particles

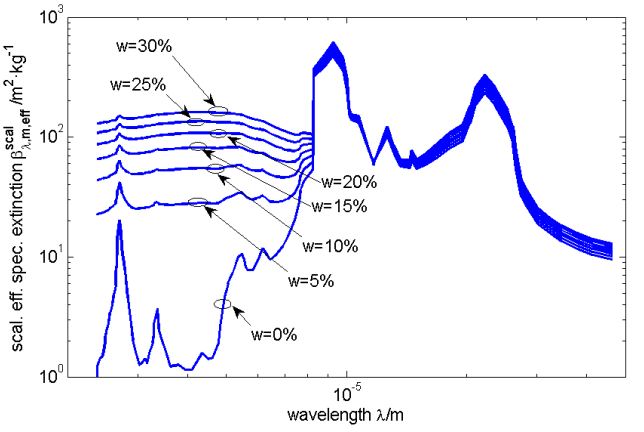

Figure 9: Dependence of the scaling effective specific extinction coefficient versus wavelength of SiC-doped silica aerogel on amount of the SiC particles

5.2.2 Thermal conductivity of the SiC particle

Fig.10 shows the thermal conductivity of bulk SiC [Touloukian (1967)] and SiC particle with radius of 1 μm at different temperatures. The longitudinal and transverse sound velocities, v_l=11400 m/s, v_t=7690 m/s [Gust et al (1973)] were used to calculated the particle thermal conductivity. As shown that the thermal conductivity of the particle is far less than that of the bulk material, because the MFP of the phonons in the bulk SiC (about 272.38 μm at 300 K) is much larger than the particle size. The MFP of the phonons in the particle is mainly depends on the particle size.

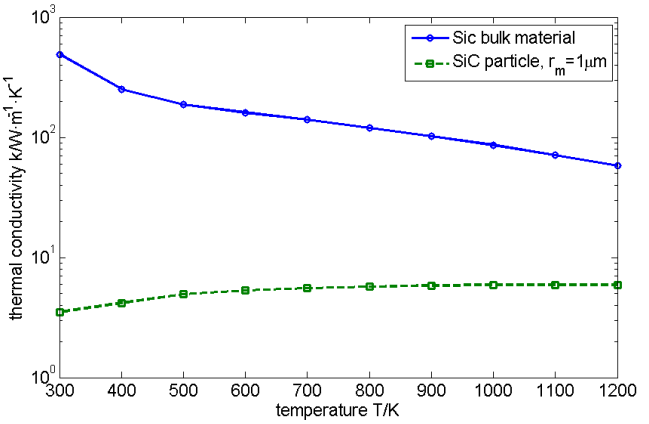

Figure 10: Dependence of thermal conductivity of bulk SiC and SiC particle versus temperature

5.2.3 Optimal doping amount of the SiC particles

Based on the calculated radiative properties and solid conductivity, the ETC of the evacuated SiC-doped silica aerogel was computed. Fig. 11 shows the variation of the thermal conductivity versus the doping amount of the particles. The density of the silica aerogel matrix is 114 kg/m^3 and the cold wall temperature was set to 333.15 K, the hot wall temperature was set to 473.15, 773.15, 1073.15 K, corresponding to the low, medium and high temperature conditions, respectively. It can be seen that as the doping amount of the particles increases, the ETC decreases rapidly at first and then changes gently. It obtains a minimum value at somewhere, and then increases slowly. When the hot wall temperature is 473.15 K, the optimal doping amount is about 15%, and the minimum ETC is about 0.0074 W/(m·K). When the hot wall temperature is 773.15 K, the optimal doping amount is about

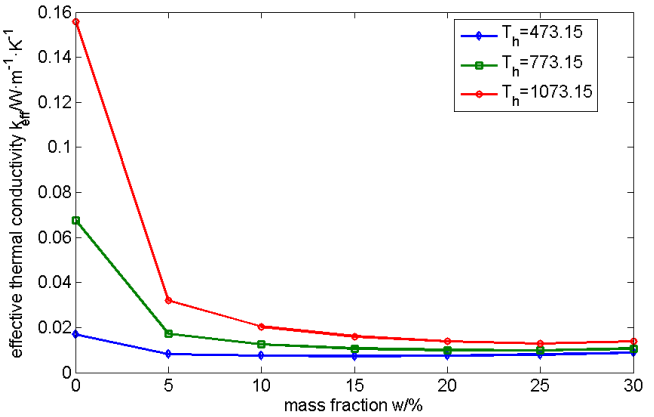

Figure 11: Dependence of the ETC of evacuated SiC-doped silica aerogel versus doping amount at different hot wall temperatures

20%, and the minimum ETC is about 0.0099 W/(m·K). When the hot wall temperature is 1073.15 K, the optimal doping amount is about 25%, and the minimum ETC is about 0.0128 W/(m·K). The results show that the optimal doping amount of the opacifier increases as the temperature increases.

6 Conclusion

In this paper, a theoretical model was proposed to investigate the radiative properties and the ETC of the opacified silica aerogel. This model can be readily used for finding efficient opacifier and determining the optimal parameters for the opacifier. This may be useful for the thermal insulation material design.

The radiative properties of the TiO_2-doped silica aerogel with different doping amount were calculated. The calculated results are found to be close to the experimental results. It is also found that, doping particles to the aerogel matrix will introduce a forward scattering and the particle size distribution can affect the effective extinction coefficient. The ETC of the 30% TiO_2-doped silica aerogel were calculated. The calculated values were compared with the experimental values and a maximum relative difference of 12.4% is observed. The difference may be attributed to the effect of dependent scattering caused by the ceramic fiber in the experimental material.

The thermophysical properties of the SiC-doped silica aerogel were also calculated. It is found that the optimal mean radius of the SiC particles for the largest radiation extinction is about 1μm. The optimal doping amount of the SiC particles for the

evacuated silica aerogel is about 15%, 20% and 25%, corresponding to the low, medium and high temperature conditions, respectively.

Acknowledgement

This work was supported by the New Century National Excellent Talents Program through the Ministry of Human Resource and Social Security of China, as well as by the New Century Excellent Talents Program in University, funded by the Ministry of Education of China. The authors are also pleased to acknowledge the support of Professor S.N. Atluri of University of California, Irvine.

References

Akimov, Y. K. (2003): Fields of application of aerogels (Review). *Instrum Exp Tech*, vol. 46, no. 3, pp. 287–299.

Bohren C F.; Huffman D R. (1983): *Absorption and scattering of light by small particles.* John Wiley & Sons, Inc.

Bouquerel, M.; Duforestela T.; Baillis, D.; Rusaouen, G. (2012): Heat transfer modeling in vacuum insulation panels containing nanoporous silicas—a review. *Energ Buildings*, vol. 54, pp. 320–336.

Caravaca, M. A.; Mino, J. C.; Perez, V. J.; Casali, R. A.; Ponce, C. A. (2009): Ab initio study of the elastic properties of single and polycrystal TiO_2, ZrO_2 and HfO_2 in the cotunnite structure. *J. Phys. Condens. Matter,* vol. 21 015501-1-015501-11.

Chen, G. (2005): *Nanoscale energy transport and conversion.* Oxford university press.

Chen, W. H.; Wu, C. H.; Cheng, H. C. (2011): Temperature-dependent thermodynamic behaviors of carbon fullerene molecules at atmospheric pressure. *CMC: Computer, Materials & Continua*, vol. 25, No.3, pp.195-241.

Coquard, R.; Baillis, D.; Grigorova, V.; Enguehard, F; Quenard, D.; Levitz, P. (2013): Modeling of the conductive heat transfer through nano-structured porous silica materials. *J. Non-Cryst Solids* vol.363, pp. 103–115.

Dombrovsky, L. A. (2004): The propagation of infrared radiation in a semitransparent liquid containing gas bubbles. *High Temp*, vol. 42 pp. 143-150.

Dondero, M.; Cisilino, A. P.; Tomba, J. P. (2011): Numerical design of random micro-heterogenous materials with functionally-graded effective thermal conductivities using genetic algorithms and the fast boundary element method. *CMES: Computer Modeling in Engineering and Sciences*, vol. 78, no. 4, pp.225-245.

Dorcheh, A. S.; Abbasi, M. H. (2008): Review Silica aerogel; synthesis, properties and characterization. *J. Mater. Process Tech*, vol. 199, pp. 10–26.

Enguehard, F. (2007): Multi-scale modeling of radiation heat transfer through nanoporous superinsulating materials. *Int. J. Thermophys.,* vol.28, pp. 1693-1717.

Fu, Q.; Sun, W. b. (2001): Mie theory for light scattering by a spherical particle in an absorbing medium. *Applied optics*, vol. 40, no. 9, pp. 1354-1361.

Fricke, J.; Heinemann, U.; Ebert, H. P. (2008): Vacuum insulation panels—from research to market. *Vacuum*, vol. 82, pp. 680-690.

Fricke, J.; Tillotson, T. (1997): Aerogels: production, characterization, and applications. *Thin Solid Films*, vol.297, pp. 212–223.

Gust, W. H.; Holt, A. C.; Royce, E. B. (1973): Dynamic yield, compressional, and elastic parameters for several light weight inter metallic compounds. *J. Appl. Phys*, vol. 44, no. 2, pp. 550-560.

Han, K.; Feng, Y. T.; Owen, D. R. J. (2009): An accurate algorithm for evaluating radiative heat transfer in a randomly packed bed. *CMES: Computer Modeling in Engineering and Sciences*, vol. 49, no. 2, pp.143-161.

Huang, M. J.; Tsai, T. C.; Liu, L. C.; Jeng, M. S.; Yang, C. C. (2009): A fast monte-carlo solver for phonon transport in nanostructured semiconductors. *CMES: Computer Modeling in Engineering and Sciences*, vol. 42, no. 2, pp. 107-129.

Incropera, F. P.; DeWitt, D. P.; Bergman, T. L.; Lavine, A. S. (2007): *Fundamentals of heat and mass transfer (sixth edition)*. John Wiley & Sons, Inc.

Kuhn, J; Gleissner, T.; Arduini-schuster, M. C; Korder, S.; Fricke, J. (1995): Integration of mineral powders into SiO_2 aerogels. *J. Non-Cryst Solids*, vol. 186, pp. 291-295.

Li, D. S.; Saheli, G.; Khaleel, M.; Garmestani, H. (2006): Microstructure optimization in fuel cell electrodes using materials design. *CMC: Computer, Materials & Continua*, vol. 4, No.1, pp.31-42.

Liang, X. Y.; Yang, Z.; Gu, X. S.; Ling, L. C. (2009): Research on activated carbon supercapacitors electrochemical properties based on improved PSO-BP neural network. *CMC: Computer, Materials & Continua*, vol. 13, No.2, pp.135-152.

Liu, C. S. (2011): Using a lie-group adaptive method for the identification of a nonhomogeneous conductivity function and unknown boundary data. *CMC: Computer, Materials & Continua*, vol. 21, No.1, pp.17-40.

Lu, X.; Arduini-schuster, M. C.; Kuhn, J.; Nilsson, O.; Fricke, J.; Pekala, R.W. (1992): Thermal conductivity of monolithic organic aerogels. *Science*, vol. 255, no. 5047, pp. 971-972.

Modest, M. F. (2003): *Radiative heat transfer (second edition).* Academic Press.

Ni, J. H.; Chang, C. C.; Yang, Y. T.; Chen, C. K. (2011): Surface heating problems of thermal propagation in living tissue solved by differential transformation method. *CMES: Computer Modeling in Engineering and Sciences*, vol. 72, no. 1, pp.37-51

Pilon, L.; Viskanta, R. (2003): Radiation characteristics of glass containing bubbles. *J. Am Ceram Soc*, vol. 86, pp. 1313-1320.

Randrianalisoa, J.; Baillis, D.; Pilon, L. (2006): Modeling radiation characteristics of semitransparent media containing bubbles or particles. *J. Opt. Soc. Am. A* vol. 23, no. 7, pp. 1645-1656.

Tian, W. X.; Yang, R. G. (2008): Phonon transport and thermal conductivity percolation in random nanoparticle composites. *CMES: Computer Modeling in Engineering and Sciences*, vol. 24, no. 2, pp.123-141.

Touloukian, Y. S. (1967): *Thermophysical properties of high temperature solid material*, MacMillan Co.

Wang, J.; Kuhn, J.; Lu, X. (1995): Monolithic silica aerogel insulation doped with TiO2 powder and ceramic fibers. *J. Non-Cryst Solids*, vol. 186, pp. 296-300.

Wei, G. S.; Liu, Y. S.; Du, X. Z.; Zhang, X. X. (2012): Gaseous conductivity study on silica aerogel and its composite insulation materials. *J. Heat Trans-T ASME,* vol. 134, pp. 041301-041301-5.

Wei, G. S.; Liu, Y. S.; Zhang, X. X; Yu, F.; Du, X. Z. (2011) Thermal conductivities study on silica aerogel and its composite insulation materials. *Int. J. Heat Mass Tran.*, vol. 54, pp. 2355–2366.

Yang, P.; Gao, B. C; Wiscombe, W. J.; Mishchenko, M. I.; Platnick, S.; Huang, H. L.; Baum, B. A.; Hu, Y. X.; Winker, D.; Tsay, S. C.; Park, S. K. (2002): Inherent and Apparent Scattering Properties of Coated or Uncoated Spheres Embedded in an Absorbing Host Medium. *Appl Optics*, vol. 41, pp. 2740-2759.

Yang, Z. C.; Chen D. P. (2009): Preparation and thermal properties of silica nanoporous thermal insulation materials. *J. Chin Ceram Soc*, vol. 37, no. 10, pp. 1740-1743.

Yin, J.; Pilon, L. (2006): Efficiency Factors and radiation characteristics of spherical scatterers in absorbing media. *J. Opt. Soc. Am. A.*, vol. 23, no. 11, pp. 2784-2796.

Zeng, S. Q.; Hunt, A.; Greif, R. (1995): Geometric structure and thermal conductivity of porous medium silica aerogel. *J. Heat Trans-T. ASME*, vol. 117, pp. 1055-1058.

Zeng, S. Q.; Hunt, A.; Greif, R. (1995): Transport properties of gas in silica

aerogel. *J. Non-Cryst Solids*, vol. 186, pp. 264-270.

Zeng, S. Q.; Hunt, A.; Greif, R. (1995): Theoretical modeling of carbon content to minimize heat transfer in silica aerogel. *J. Non-Cryst Solids*, vol. 186, pp. 271-277.

Zhang, H. X.; Fang, S. Q. (2012): Preparation and heat transferring performance of TiO2/SiO2 composite aerogels. *J Harbin Eng Uni.*, vol.33, no.3, pp.1-5.

Zhao, J. J.; Duan, Y. Y.; Wang, X. D.; Wang, B. X. (2012): Radiative properties and heat transfer characteristics of fiber-loaded silica aerogel composites for thermal insulation. *Int. J. Heat Mass Tran.*, vol. 55, pp. 5196–5204.